COMMUNICATION

Construction of a Triangle-Shaped Trimer and a Tetrahedron Using an α-Helix-Inserted Circular Permutant of Cytochrome c_{555}

Akiya Oda,[a] Satoshi Nagao,[a] Masaru Yamanaka,[a] Ikki Ueda,[a] Hiroki Watanabe,[b] Takayuki Uchihashi,[b] Naoki Shibata,[c] Yoshiki Higuchi,[c] and Shun Hirota*[a]

Abstract: Highly-ordered protein structures have gained interest for future uses for biomaterials. Herein, we constructed a building block protein (BBP) by the circular permutation of the hyperthermostable *Aquifex aeolicus* cytochrome (cyt) c_{555}, and assembled BBP into a triangle-shaped trimer and a tetrahedron. The angle of the intermolecular interactions of BBP was controlled by cleaving the domain-swapping hinge loop of cyt c_{555} and connecting the original N- and C-terminal α-helices with an α-helical linker. We obtained BBP oligomers up to ~40 mers, with a relatively large amount of trimers. According to the X-ray crystallographic analysis of the BBP trimer, the N-terminal region of one BBP molecule interacted intermolecularly with the C-terminal region of another BBP molecule, resulting in a triangle-shaped structure with an edge length of 68 Å. Additionally, four trimers assembled into a unique tetrahedron in the crystal. These results demonstrate that the circular permutation connecting the original N- and C-terminal α-helices with an α-helical linker may be useful for constructing organized protein structures.

In highly-ordered protein oligomers, the subunit orientations are precisely controlled, making the oligomers suitable for various functions, such as biomolecule production, storage, and transfer.[1] Protein oligomers with unique structures have also been designed.[2] For example, polymers, nanosheets, and nanocages have been constructed by protein fusion,[3] computer design,[4] metal coordination,[5] disulfide bond,[5c,6] and chemical modification.[7] For fusion proteins, a well-defined cage structure was constructed by connecting the C-terminal α-helix of a protein with the N-terminal α-helix of another protein,[3a] whereas barrel hexamers and tetrahedral dodecamers were generated with another fusion protein.[3b] Tetrahedral and octahedral nanocages have been constructed with a trimer by designing the protein interfaces for specific interactions.[4a] Circular permutation is also effective for constructing oligomers,[8] as well as nanocages and nanoparticles.[9] Circular permutation has been originally observed in native proteins;[10] however recently, it is used to create proteins by connecting the N- and C-termini of a protein and cleaving the peptide bond at an arbitrary position.[11] For example, circular permutation has been performed for the hexameric PduA shell protein, resulting in formation of a pentameric cage smaller than the native cage.[9a]

We have previously reported 3D domain swapping (here domain swapping) oligomerization of various heme proteins.[12] A cage structure was constructed with three domain-swapped dimers of cytochrome (cyt) cb_{562}, a *c*-type cyt of cyt b_{562},[12e] whereas a protein nanoring of *Hydrogenobacter thermophilus* cyt c_{552} was constructed by extending the hinge loop of domain swapping.[12g] *Aquifex aeolicus* (AA) cyt c_{555} is a hyperthermostable *c*-type cyt, which is different from other *c*-type cyts by possessing an extra α-helix at the heme-coordinating Met site.[13] AA cyt c_{555} exhibits high thermostablity (denaturing temperature, 130 °C), owing to the tight packing of the amino acids in the protein interior.[14] AA cyt c_{555} forms a domain-swapped dimer by exchanging the C-terminal region between molecules, where the Val53–Lys57 region acts as a hinge loop.[12h] In this study, to construct a stable protein oligomer by enhancing the intermolecular interaction of the N-terminal of a protein molecule with the C-terminal region of another protein molecule, we constructed a building block protein (BBP) based on AA cyt c_{555} circular permutation: AA cyt c_{555} was cleaved at the hinge loop between Ile52 and Val53, and the original N- and C-terminal α-helices were connected with an α-helix linker (Figure 1). Oligomers were formed by drying the BBP solution at 80 ºC and subsequently re-dissolving the residual. The trimer exhibited a closed triangle structure, and four of these BBP trimers formed a tetrahedron in the crystal.

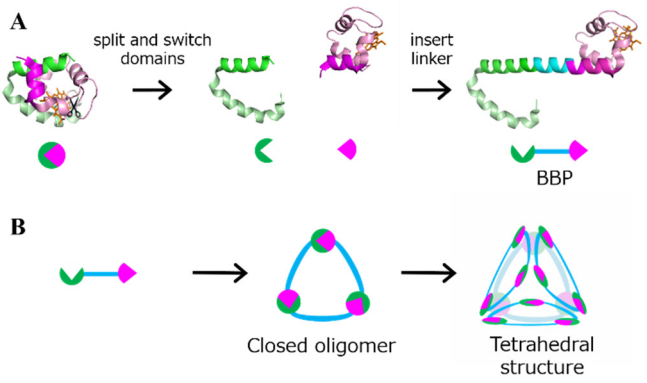

Figure 1. Schematic representation of BBP design and its oligomerization: (A) Circular permutation of AA cyt c_{555} with the connection of the original N- and C-terminal α-helices with an α-helix linker, (B) formation of a trimer and a tetrahedron. N- and C-terminal regions of AA cyt c_{555} are depicted in magenta and green, respectively. The hemes are shown as orange stick models in the protein structures.

[a] A. Oda, Dr. S. Nagao, Dr. M. Yamanaka, I. Ueda, Prof. Dr. S. Hirota
Graduate School of Materials Science
Nara Institute of Science and Technology
8916-5 Takayama, Ikoma, Nara 630-0192, Japan
E-mail: hirota@ms.naist.jp
[b] Dr. H. Watanabe, Prof. Dr. T. Uchihashi
Department of Physics, Nagoya University
Chikusa-ku, Nagoya, Aichi 464-8602, Japan
[c] Dr. N. Shibata, Prof. Dr. Y. Higuchi
Department of Life Science, Graduate School of Life Science,
University of Hyogo, 3-2-1 Koto, Kamigori-cho, Ako-gun, Hyogo 678-1297, Japan
RIKEN SPring-8 Center, 1-1-1 Koto, Sayo-cho, Sayo-gun, Hyogo 679-5148, Japan

Supporting information for this article is given via a link at the end of the document.

The N- and C-terminal α-helices interact with a defined angle (~ 91°) in AA cyt c_{555} (Figure S1 in the Supporting Information). Since connecting the N- and C-terminal α-helices with an α-helix is useful to fix the orientation of intermolecular interaction,[3a] we envisaged that the intermolecular interaction is enhanced and the intermolecular orientations are controllable by circular permutation, connecting the original N- and C-terminal α-helices with an α-helix linker (Figure 1A). Circular permutation of AA cyt c_{555} was performed at the hinge loop (between Ile52 and Val53) of domain swapping. The α-helix linker consisted of nine amino acids. The amino acid sequence of the linker and three modified amino acids at the original N- and C-termini (RIAKQAQEKQQQDVA, Table S1) was based on the α-helix linker sequence reported for a fusion protein forming a 24 mer cage[15] with the following modifications: An additional Ala was added to the linker, adjusting the dihedral angle between two BBP molecules to be near 0°. Hydrophobic amino acids were introduced at the positions of the amino acids that were expected to be close to the hydrophobic site of the AA cyt c_{555}-originated unit. Five amino acids in the linker were modified to form electrostatic interactions and hydrogen bonds between the linkers of different protomers, when BBP forms an oligomer. Finally, three amino acids at the original N- and C-termini were modified to remove the steric hindrances between the linkers of different protomers.

BBP was purified as a monomer from an *E. coli* expression system, and oligomerized by drying the monomer solution at 80 °C and re-dissolving the residual with pure water (Figure S2). The sizes of the BBP oligomers were analysed by size exclusion chromatography, indicating that the BBP oligomers up to about 40 mer were constructed. A relatively large amount of trimers were obtained, and the trimer was subsequently purified by size exclusion chromatography and ion exchange chromatography. By incubation of the BBP trimer solutions at 50 °C for 30 min, more than half of the trimers dissociated to monomers and dimers, whereas most of the BBP trimers did not by incubation at 40 °C for 30 min, showing that the BBP trimer is stable below 40 °C (Figure S3).

The optical absorption and circular dichroism (CD) spectra of the BBP monomer and trimer were measured to obtain information in the solution structures (Figure S4). AA cyt c_{555} (monomer), BBP monomer, and BBP trimer exhibited Soret bands at 412, 407, and 408 nm, with absorption coefficients of 122,000, 124,000, and 128,000 M^{-1} cm^{-1}, respectively. The absorbance around 695 nm, which is attributed to the Fe–Met bond, was detected in the absorption spectra of AA cyt c_{555}, BBP monomer, and BBP trimer; however, the intensities of the 695-nm band of the BBP monomer and trimer were decreased 52% and 36%, respectively, compared to that of AA cyt c_{555}. The wavelengths of the Soret bands of the BBP monomer and trimer blue-shifted to 407 and 408 nm, respectively, from that of AA cyt c_{555} (412 nm). These properties indicate that both the BBP monomer and trimer exist in equilibriums between Met coordination and dissociation from the heme iron; the Met coordination ratio in the BBP trimer being higher than that in the BBP monomer, judging from the Soret wavelengths. The methionine coordination to the heme iron may stabilize the BBP trimer, since for horse cyt *c* the methionine coordination to the heme iron affects the stability of the domain-swapped dimer, but does not influence the oligomer formation amount, probably because the oligomers are kinetically trapped.[12j]

Negative Cotton effects were observed at 208 and 222 nm in the CD spectra of AA cyt c_{555}, BBP monomer, and BBP trimer solutions. The intensities of the Cotton effect were similar between the spectra of AA cyt c_{555} and BBP monomer, indicating that the two proteins possess similar α-helical ratio. Since BBP comprises nine more amino acids than AA cyt c_{555}, the CD results indicate that there are more α-helices in the BBP monomer compared to that in AA cyt c_{555}; and thus, the introduced linker may partially fold into an α-helix in the BBP monomer. However, the intensities of the Cotton effect at 208 and 222 nm were larger for the spectrum of the BBP trimer compared to that of the BBP monomer, indicating that the α-helical amount in BBP increased by the conversion from the monomer to trimer. The CD spectrum of the BBP monomer at 100 ºC did not exhibit a significant difference from that at 25 ºC, indicating that the BBP monomer is very stable, as native AA cyt c_{555} (denaturation temperature: ~130 ºC[14]) (Figure S4B).

High-speed atomic force microscopy (HS-AFM) observation of the BBP trimer was performed to characterize its structural stability (Figure 2 and Movie S1). The BBP trimer was mainly in a closed cyclic structure; however, the closed trimer structure occasionally converted to open structures for short periods (4.1–4.4 s; 44.3–44.7 s; 45.1–45.9 s in Figure 2), where it returned relatively quickly to the closed structure. These results indicate a dynamic feature for the BBP trimer, where the fluctuation character of the trimer may induce formation of higher-order oligomers.

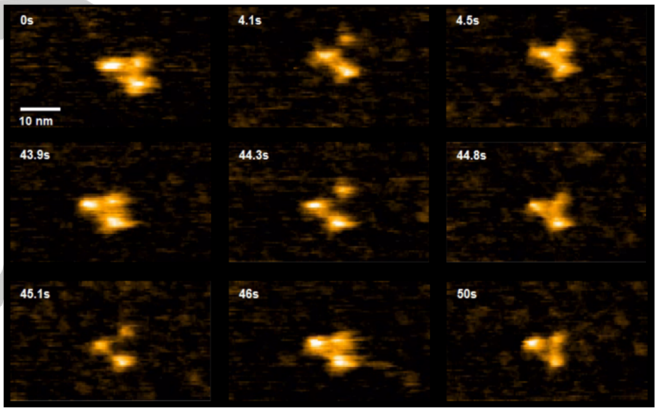

Figure 2. Clipped HS-AFM images of the BBP trimer adsorbed on the APTES-mica. HS-AFM images were captured with a frame rate of 10 fps for 50 s.

X-ray crystallographic analysis of the BBP trimer was performed to elucidate the detailed structure. The BBP trimer structure was obtained at 1.7 Å resolution (PDB ID: 5Z25) (Figure 3A), where one BBP molecule existed in the asymmetric unit of the BBP trimer crystal. The N-terminal region of a BBP molecule interacted intermolecularly with the C-terminal region of another BBP molecule, resulting in the formation of a triangle-shaped structure with an edge length of 68 Å. In the BBP trimer, a CH−π interaction between Phe30 and Ile34 existed within each protomer, and the α-helix linker was bent 50.1° at Leu32–Ile34 (Figure S5). Phe30 and Ile34 may locate close when the linker forms an α-helix, allowing these amino acids interact between each other. The linker may have maintained the α-helix around the bent Leu32–Ile34 region, owing to the relatively high α-helical propensities for the amino acids at the bent region.[16] The radius of gyration of the BBP trimer (24.7 Å), calculated from its X-ray crystal structure (PDB ID 5Z25), was similar to that estimated from

size exclusion chromatography (21.5 Å) (Figure S2B), indicating that the BBP trimer may form a closed structure also in solution. According to the CD and X-ray crystallographic analyses, only a part of the linker may form an α-helix for the monomer, whereas the whole linker region converts to an α-helix in the trimer. The three dimensional structure of the globular unit formed by the interaction of the N-terminal region of one protomer and the C-terminal region of another protomer was similar to that of AA cyt c_{555} (PDB ID: 5Z25 and 2ZXY) (Figure S6). The root-mean-square deviation (rmsd) value was 0.97 Å for the Cα atoms between AA cyt c_{555} and the corresponding region in the globular unit of the BBP trimer, where the residues in the hinge loop (Val53–Lys57) and three residues at the N- and C-termini of AA cyt c_{555} were excluded. Thus, the BBP trimer was relatively stable, owing to the high hydrophobic packing of the AA cyt c_{555} globular unit in the trimer, similar to that of AA cyt c_{555}. (Figure S3).

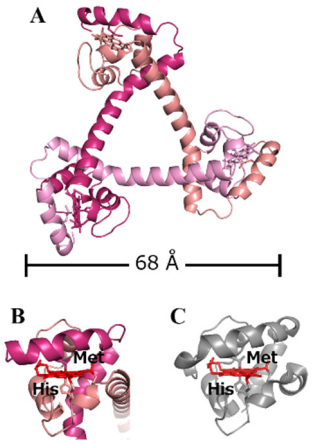

Figure 3. (A) Crystal structure of BBP trimer (PDB ID: 5Z25). The violet, red purple, and pink regions represent different protomers. The scale bar corresponds to the distance between the Cα atom of Gly18 in one protomer (red purple) and that of Ala4 in another protomer (pink). (B) Active site structure of the BBP trimer (PDB ID: 5Z25). (C) Active site structure of AA cyt c_{555} (PDB ID: 2ZXY). The hemes are depicted in red for the active site structures (B and C). The hemes and heme-coordinating residues (Met and His) are shown as stick models.

Met coordinated to the heme iron in the BBP trimer as in AA cyt c_{555}, but it originated from the other protomer to which the heme belonged (Figure 3B). The Fe−His and Fe−Met distances in the BBP trimer were 2.11 and 2.27 Å, respectively, which were similar to the corresponding distances in AA cyt c_{555} (Fe−His, 2.00 Å; Fe−Met, 2.30 Å).[13] According to the Soret band wavelength shifts, Met coordination to the heme iron was cleaved in some of the globular units of the BBP trimers in solution (Figure S4A). Although Met was coordinated to the heme iron for the BBP trimer in the crystal, an equilibrium between Met coordination and dissociation existed in solution for the BBP trimer.

It is noteworthy that four BBP trimers packed into a tetrahedron in the crystal (Figure 4). Hydrogen bonds between the Nζ atom of Lys54 of a BBP trimer and the main chain O atom of Ser58 of another BBP trimer, and between the Oε1 atom of Gln53 of a BBP trimer and the Nε2 atom of Gln61 of another BBP trimer were formed in the tetrahedron (Lys54(Nζ)–Ser58(O), 3.0 Å; Gln53(Oε1)–Gln61(Nε2), 3.1 Å) (Figure S7). There are twelve protomers in the tetrahedron, and thus the tetrahedral packing was stabilized with 24 hydrogen bonds. Additionally, there was a PEG molecule (tetraethylene glycol, $C_8H_{18}O_5$) sitting at each vertex of the tetrahedron (Figure S8). Eight tetrahedrons were packed in the unit cell, in which hydrogen bonds between Val1 of a trimer of a tetrahedron and Glu92 of a trimer of another tetrahedron were formed (Figure S9). Although the tetrahedron was not stable in solution, introductions of metal coordination and disulfide bond at the interfaces of the trimers may be useful to stabilize the tetrahedral packing.[5-6]

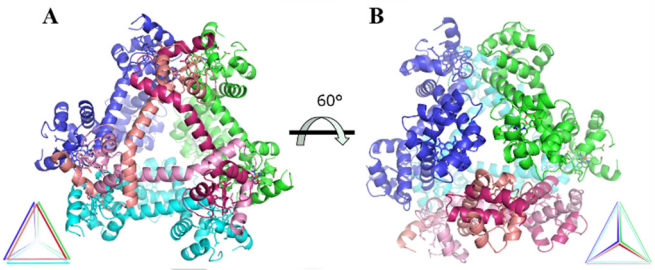

Figure 4. Tetrahedron constructed with four BBP trimers in the crystal (PDB ID: 5Z25). Each trimer forming the tetrahedron is shown in green, pink, cyan, and blue, respectively. (B) is a 60°-rotated view of (A). Schematic illustrations are shown at the lower left and right corners.

Tetrahedrons constructed by computational design and fusion proteins have edges longer than 100 Å.[3b,4a,17] Ni *et al.* reported a crystalline tetrahedral cage with an edge length of about 80 Å using a cyt cb_{562} surface mutant coordinated to zinc ions,[18] whereas Gradišar *et al.* constructed a tetrahedron with that about 70 Å utilizing a single polypeptide chain with twelve coiled coil-forming segments.[19] A relatively short edge length was achieved for the BBP tetrahedron owing to the circular permutation of a relatively small protein.

Protein fusion[3b,15] and circular permutation[9] of oligomeric proteins have been utilized as building blocks for highly-ordered protein structures. For a fusion protein, it contains at least two units, and the fusion protein may become large, making it difficult to control the overall structure and create small highly-ordered structures. In circular permutation, the linker of the original N- and C-termini may form a loop, making it difficult to control the orientation and association of the structural units. In the present study, the orientations between the proteins (protomers) are fixed by performing circular permutation and connecting the original N- and C-terminal α-helices with an α-helix, allowing formation of a closed triangle-shaped trimer and a relatively small tetrahedron. Other highly-ordered structures may be constructed by adjusting the length and amino acids at the α-helix linker.

In conclusion, a building block protein, BBP, was constructed by circular permutating AA cyt c_{555} at the hinge loop of domain swapping and connecting the original N- and C-terminal α-helices with an α-helical linker. The BBP trimer exhibited a closed triangle structure, where the inserted linker formed an α-helix. Additionally, four BBP trimers formed a tetrahedron in the crystal. The present method utilizes circular permutation of a thermostable protein possessing α-helices at the N- and C-terminal regions, which is suitable for constructing small organized protein structures.

Acknowledgements

The synchrotron radiation experiments were performed at the BL38B1 beamline of SPring-8 with the approval of JASRI (No. 2016A2730; S.N.). This work was partially supported by Grants-

in-Aid from JSPS for Scientific Research (Category B, No. JP26288080 (S.H.); Challenging Exploratory Research, No. JP15K13744 (S.H); Innovative Areas, No. JP16H00839 (S.H.), No. JP16H00830 (T.U.) and JP16H00758 (T.U.)).

Keywords: protein design • circular permutation • cytochrome c_{555} • protein oligomer • protein structures

[1] B. J. G. E. Pieters, M. B. van Eldijk, R. J. M. Nolte, J. Mecinovic, *Chem. Soc. Rev.* **2016**, *45*, 24-39.

[2] a) K. Matsuurua, *RSC Adv.* **2014**, *4*, 2942-2953; b) Q. Luo, C. X. Hou, Y. S. Bai, R. B. Wang, J. Q. Liu, *Chem. Rev.* **2016**, *116*, 13571-13632.

[3] a) Y. T. Lai, D. Cascio, T. O. Yeates, *Science* **2012**, *336*, 1129; b) N. Kobayashi, K. Yanase, T. Sato, S. Unzai, M. H. Hecht, R. Arai, *J. Am. Chem. Soc.* **2015**, *137*, 11285-11293; c) A. Sciore, M. Su, P. Koldewey, J. D. Eschweiler, K. A. Diffley, B. M. Linhares, B. T. Ruotolo, J. C. Bardwell, G. Skiniotis, E. N. Marsh, *Proc. Natl. Acad. Sci. USA* **2016**, *113*, 8681-8686; d) T. O. Yeates, *Ann. Rev. Biophys.* **2017**, *46*, 23-42; e) S. Badieyan, A. Sciore, J. D. Eschweiler, P. Koldewey, A. S. Cristie-David, B. T. Ruotolo, J. C. A. Bardwell, M. Su, E. N. G. Marsh, *Chembiochem* **2017**, *18*, 1888-1892.

[4] a) N. P. King, W. Sheffler, M. R. Sawaya, B. S. Vollmar, J. P. Sumida, I. Andre, T. Gonen, T. O. Yeates, D. Baker, *Science* **2012**, *336*, 1171-1174; b) P. S. Huang, S. E. Boyken, D. Baker, *Nature* **2016**, *537*, 320-327.

[5] a) Y. Bai, Q. Luo, W. Zhang, L. Miao, J. Xu, H. Li, J. Liu, *J. Am. Chem. Soc.* **2013**, *135*, 10966-10969; b) T. Sendai, S. Biswas, T. Aida, *J. Am. Chem. Soc.* **2013**, *135*, 11509-11512; c) Y. Suzuki, G. Cardone, D. Restrepo, P. D. Zavattieri, T. S. Baker, F. A. Tezcan, *Nature* **2016**, *533*, 369-373.

[6] E. R. Ballister, A. H. Lai, R. N. Zuckermann, Y. Cheng, J. D. Mougous, *Proc. Natl. Acad. Sci. USA* **2008**, *105*, 3733-3738.

[7] a) S. Burazerovic, J. Gradinaru, J. Pierron, T. R. Ward, *Angew. Chem. Int. Ed.* **2007**, *46*, 5510-5514; b) H. Kitagishi, K. Oohora, H. Yamaguchi, H. Sato, T. Matsuo, A. Harada, T. Hayashi, *J. Am. Chem. Soc.* **2007**, *129*, 10326-10327; c) D. Sicard, S. Cecioni, M. Iazykov, Y. Chevolot, S. E. Matthews, J. P. Praly, E. Souteyrand, A. Imberty, S. Vidal, M. Phaner-Goutorbe, *Chem. Commun.* **2011**, *47*, 9483-9485.

[8] Z. Qian, J. R. Horton, X. Cheng, S. Lutz, *J. Mol. Biol.* **2009**, *393*, 191-201.

[9] a) J. Jorda, D. J. Leibly, M. C. Thompson, T. O. Yeates, *Chem. Commun.* **2016**, *52*, 5041-5044; b) N. Kawakami, H. Kondo, M. Muramatsu, K. Miyamoto, *Bioconjugate Chem.* **2017**, *28*, 336-340.

[10] B. A. Cunningham, J. J. Hemperly, T. P. Hopp, G. M. Edelman, *Proc. Natl. Acad. Sci. USA* **1979**, *76*, 3218-3222.

[11] Y. Yu, S. Lutz, *Trends Biotechnol.* **2011**, *29*, 18-25.

[12] a) S. Hirota, Y. Hattori, S. Nagao, M. Taketa, H. Komori, H. Kamikubo, Z. Wang, I. Takahashi, S. Negi, Y. Sugiura, M. Kataoka, Y. Higuchi, *Proc. Natl. Acad. Sci. USA* **2010**, *107*, 12854-12859; b) Y. Hayashi, S. Nagao, H. Osuka, H. Komori, Y. Higuchi, S. Hirota, *Biochemistry* **2012**, *51*, 8608-8616; c) S. Nagao, H. Osuka, T. Yamada, T. Uni, Y. Shomura, K. Imai, Y. Higuchi, S. Hirota, *Dalton Trans.* **2012**, *41*, 11378-11385; d) Y. W. Lin, S. Nagao, M. Zhang, Y. Shomura, Y. Higuchi, S. Hirota, *Angew. Chem. Int. Ed.* **2015**, *54*, 511-515; e) T. Miyamoto, M. Kuribayashi, S. Nagao, Y. Shomura, Y. Higuchi, S. Hirota, *Chem. Sci.* **2015**, *6*, 7336-7342; f) S. Nagao, M. Ueda, H. Osuka, H. Komori, H. Kamikubo, M. Kataoka, Y. Higuchi, S. Hirota, *Plos One* **2015**, *10*, e0123653; g) C. G. Ren, S. Nagao, M. Yamanaka, H. Komori, Y. Shomura, Y. Higuchi, S. Hirota, *Mol. Biosyst.* **2015**, *11*, 3218-3221; h) M. Yamanaka, S. Nagao, H. Komori, Y. Higuchi, S. Hirota, *Protein Sci.* **2015**, *24*, 366-375; i) M. Yamanaka, M. Hoshizumi, S. Nagao, R. Nakayama, N. Shibata, Y. Higuchi, S. Hirota, *Protein Sci.* **2017**, *26*, 464-474; j) S. Hirota, N. Yamashiro, Z. Wang, S. Nagao, *J Biol Inorg Chem* **2017**, *22*, 705-712.

[13] M. Obuchi, K. Kawahara, D. Motooka, S. Nakamura, M. Yamanaka, T. Takeda, S. Uchiyama, Y. Kobayashi, T. Ohkubo, Y. Sambongi, *Acta Crystallogr. D. Biol. Crystallogr.* **2009**, *65*, 804-813.

[14] a) M. Yamanaka, H. Mita, Y. Yamamoto, Y. Sambongi, *Biosci. Biotech. Biochem.* **2009**, *73*, 2022-2025; b) M. Yamanaka, M. Masanari, Y. Sambongi, *Biochemistry* **2011**, *50*, 2313-2320.

[15] Y. T. Lai, E. Reading, G. L. Hura, K. L. Tsai, A. Laganowsky, F. J. Asturias, J. A. Tainer, C. V. Robinson, T. O. Yeates, *Nat. Chem.* **2014**, *6*, 1065-1071.

[16] J. W. Bryson, S. F. Betz, H. S. Lu, D. J. Suich, H. X. Zhou, K. T. O'Neil, W. F. DeGrado, *Science* **1995**, *270*, 935-941.

[17] a) J. E. Padilla, C. Colovos, T. O. Yeates, *Proc. Natl. Acad. Sci. USA* **2001**, *98*, 2217-2221; b) Y. T. Lai, K. L. Tsai, M. R. Sawaya, F. J. Asturias, T. O. Yeates, *J. Am. Chem. Soc.* **2013**, *135*, 7738-7743.

[18] T. W. Ni, F. A. Tezcan, *Angew. Chem. Int. Ed.* **2010**, *49*, 7014-7018.

[19] H. Gradišar, S. Božič, T. Doles, D. Vengust, I. Hafner-Bratkovič, A. Mertelj, B. Webb, A. Šali, S. Klavžar, R. Jerala, *Nat. Chem. Biol.* **2013**, *9*, 362-366.

Contents

Materials and Methods p. S2

Table S1. DNA and amino acid sequences of BBP. p. S6

Table S2. Statistics of data collection and structure refinement of the BBP trimer. p. S7

Figure S1. Interaction between the N- and C-terminal α-helices of AA cyt c_{555}. p. S8

Figure S2. Size exclusion chromatograms of BBP after oligomerization and standard proteins. p. S9

Figure S3. Size exclusion chromatograms of the BBP trimer after incubation. p. S10

Figure S4. Optical absorption and CD spectra of AA cyt c_{555}, BBP monomer, and BBP trimer. p. S11

Figure S5. Bending region in the α-helix linker of the BBP trimer. p. S12

Figure S6. Overlapped view of the BBP trimer globular unit and AA cyt c_{555}. p. S13

Figure S7. Hydrogen bonds between different BBP trimers in the tetrahedron. p. S14

Figure S8. $F_o - F_c$ omit map of the PEG molecule ($C_8H_{18}O_5$) at the vertex of the tetrahedron. p. S15

Figure S9. Packing of the tetrahedrons in the unit cell. p. S16

Movie S1. HS-AFM movie of the BBP trimer on an APTES-treated mica substrate. p. S17

Materials and Methods

Purification of BBP

Plasmid DNA of the circular permutant of AA cyt c_{555} cleaved between Ile52 and Val53 with an additional Gly at the junction of the original N- and C-termini was purchased from Eurofins genomics (Tokyo, Japan). The BBP gene was amplified by polymerase chain reaction (PCR) and sub-cloned separately into the *Eco*RI−*Sal*I site of the pKK223-3 plasmid.[1] The plasmid DNA was enhanced with *E. coli* DH5α cells, and transformed into *E. coli* JCB387 containing the pEC86 plasmid DNA.[2] The pEC86 plasmid DNA contained the cytochrome *c* maturation (ccm) genes. For substitution of Ala1Asp2Gly3 and Ser85His86Lys87 of AA cyt c_{555} to AspValAla and ArgIleAla, respectively, and insertion of LysGlnAlaGlnGluLysGlnGlnGln into the junction of the original N- and C-termini, PCR-based mutagenesis of the plasmid was performed with forward (5′-AAACAGCAGCAGGATGTGGCGAAAGCGATCTTTCAGCA-3′) and reverse (5′-TTCCTGCGCCTGTTTCGCAATGCGCAGAATGAAGTCTGCTAA-3′) primers (Eurofins genomics) using a KOD Plus mutagenesis kit (TOYOBO). DNA sequencing of mutant plasmids was conducted with a BigDye Terminator version 3.1 cycle sequencing kit (Thermo Fisher Scientific, Waltham, MA) and an ABI PRISM 3100 genetic analyzer sequencing system (Applied Biosystems, Inc. Foster City, CA). The DNA and amino acid sequences of BBP are shown in Table S1.

BBP was expressed in *E. coli* JCB387. All growths were performed aerobically in LB medium initially at 30 °C for 24 h. The cultured *E. coli* cells were harvested by centrifugation (8,000 g, 5 min, 4 °C). The cells were suspended with 100 mM Tris-HCl buffer, pH 7.0, containing 10 mM EDTA and 20% (w/v) sucrose, subsequently incubated on ice for 15 min, and centrifuged (13,700 g, 10 min, 4 °C). Then, the cells were suspended with pure water, subsequently incubated on ice for 15 min, and centrifuged (13,700 g, 10 min, 4 °C). The supernatant was dialyzed overnight at 4 °C with 25 mM sodium acetate buffer, pH 5.0. Oxidized BBP was prepared by an addition of excess (~10 fold to heme concentration) potassium ferricyanide (Wako) to the protein solution. BBP was purified by a cation exchange column (CM-cellulose, Wako) with a gradient of 0 to 250 mM NaCl. After dialysis with 25 mM sodium acetate buffer, pH 5.0, BBP was further purified with a cation exchange column (HiTrap SP, GE Healthcare) using a fast protein liquid chromatography (FPLC) system (NaCl concentration gradient, 0−300 mM; flow rate, 1.5 mL/min; monitoring wavelength, 280 nm; solvent, 25 mM sodium acetate buffer, pH 5.0, temperature, 4 °C; AKTA prime plus, GE Healthcare), and a gel filtration column (HiLoad 26/60 Superdex 75, GE Healthcare) using the FPLC system (flow rate, 2.5 mL/min; monitoring wavelength, 280 nm; solvent, 50 mM potassium phosphate buffer, pH 7.0; temperature, 4 °C). The purity of the protein was checked with SDS-PAGE. The MALDI-TOF mass spectrum of the purified BBP solution was obtained with an Autoflex II mass spectrometer (Bruker Daltonics) using sinapinic acid as a matrix in linear mode. The

absorption coefficient of the BBP monomer (ε = 124,000 ± 1,000 $M^{-1}cm^{-1}$ at 407 nm) was obtained by the pyridine hemochrome method.[3]

Preparation of the BBP trimer

The purified BBP solution was dried at 80°C, and the residual was dissolved in pure water at room temperature. The dissolved solution was analysed with a gel filtration column (HiLoad 26/600 Superdex 200 pg column, GE Healthcare) using the FPLC system (flow rate, 2.5 mL/min; monitoring wavelength, 280 nm; solvent, 50 mM potassium phosphate buffer, pH 7.0; temperature, 4 °C; AKTA prime plus, GE Healthcare). The buffer of the fraction containing the BBP trimer was exchanged with 25 mM sodium acetate buffer, pH 5.0, using an ultrafiltration tube (Amicon, molecular weight cut off of 3,000 Da, Merck Millipore). The obtained solution was purified with a cationic exchange column (Mono S™ 5/50 GL column, GE Healthcare) using the FPLC system (Biologic DuoFlow 10, Bio-rad) (flow rate, 0.5 mL/min; monitoring wavelength, 410 nm; solvent, 25 mM sodium acetate buffer, pH 5.0; temperature, 4 °C) with a NaCl concentration gradient (0−170 mM) twice. Purification of the BBP trimer from the monomer and other sizes of oligomers was confirmed by gel filtration (HiLoad 26/600 Superdex 200 pg column, GE Healthcare) using the FPLC system (flow rate, 2.5 mL/min; monitoring wavelength, 280 nm; solvent, 50 mM potassium phosphate buffer, pH 7.0; temperature, 4 °C; AKTA prime plus, GE Healthcare). The protein concentration was calculated from the absorbance of the Soret band using the coefficients of the oxidized BBP trimer (ε = 128,000 ± 1,000 $M^{-1}cm^{-1}$ at 408 nm) obtained by the pyridine hemochrome method.[3]

Analysis with size exclusion chromatography

The stability of the BBP trimer was analyzed with a Superdex 75 10/300 GL gel filtration column (GE Healthcare) using the FPLC system (flow rate, 0.5 mL/min; monitoring wavelength, 410 nm; solvent, 50 mM potassium phosphate buffer, pH 7.0; temperature, 4 °C; Biologic DuoFlow 10, Bio-rad) before and after incubation of the BBP trimer solution for 30 min at 40 and 50 °C.

The calibration curve of the radius of gyration for the HiLoad 26/60 Superdex 200 pg column was obtained using cyt *c* from horse heart (WAKO), albumin from chicken egg white (Aldrich), bovine serum albumin (BSA, Aldrich), aldolase from rabbit muscle (WAKO), and horse L-chain apoferritin lacking eight N-terminal amino acid residues[4] as standard proteins. The radii of gyration were estimated from the crystal structures (PDB ID: cyt *c* from horse heart, 1HRC; albumin from chicken egg white, 1OVA; BSA, 3V03; aldolase from rabbit muscle, 1ADO; horse L-chain apoferritin, 2ZA8) using the program, PDBparam.[5]

Optical absorption and CD measurements

Optical absorption spectra were measured with a UV-2450 spectrophotometer (Shimadzu, Japan) using a 1-cm-path-length quartz cell at 25 °C. Circular dichroism (CD) spectra were measured with a J-725 CD spectropolarimeter (Jasco, Japan) using a 0.1-cm-path-length quartz cell at 25 or 100 °C.

The concentrations of the BBP monomer and trimer were calculated from the absorbances at 407 and 408 nm, respectively, and adjusted to desired concentrations. Proteins were prepared in 50 mM potassium phosphate buffer, pH 7.0, at 7 and 50 μM (heme unit) for absorption measurements and 18 μM (heme unit) for CD measurements.

X-ray crystallographic analysis

Crystallization of the BBP trimer was carried out at 4 °C using the sitting drop vapor diffusion method with crystal plates (CrystalClear D Strips, Douglas Instruments, Hampton Research, CA). The oxidized BBP trimer was dissolved in 10 mM HEPES buffer, pH 7.0, at protein concentrations of 11 mg/mL. Droplets prepared by mixing 1 μL the BBP trimer solution with 1 μL reservoir solution were equilibrated. The best reservoir solution for the crystallographic analysis was 2.0 M ammonium sulfate with 2% (v/v) PEG 400 in 100 mM HEPES buffer, pH 7.5. Crystals were observed after incubation at 4 °C for five months.

The diffraction data were collected at the BL38B1 beamline at SPring-8, Japan. The crystal of the BBP trimer without a treatment of a cryoprotectant was mounted on a cryo-loop and flash-frozen in liquid nitrogen. The detector was MX225HE (Rayonix). The crystal-to-detector distances was 150 mm. The wavelength was 1.0000 Å, the oscillation angle was 0.5°, and the exposure time was 2.0 s per frame. The total number of frames was 180. The diffraction data were processed using the program, HKL2000.[6] The preliminary structure was obtained by a molecular replacement method (MOLREP) using the atomic coordinates of the structures of monomeric *Aquifex aeolicus* cyt c_{555} (PDB ID: 2ZXY) as a starting model. There was one BBP molecule in the asymmetric unit of the BBP trimer crystal. The structure refinement was performed using the program, REFMAC.[7] The molecular models were manually corrected, and water molecules were picked up in the electron density maps using the program, COOT.[8] The data collection and refinement statistics are summarized in Table S2.

High-speed atomic force microscopy

AFM images shown in the article were capture by a laboratory-built HS-AFM operated with tapping mode. For the HS-AFM imaging, a small cantilever with dimensions of 7-μm long, 2-μm wide, and 90-nm thick was used (AC-7, Olympus). Its nominal spring constant and resonant frequency were ~0.2 N/m and ~800 kHz, respectively, in a liquid. An amorphous carbon tip was deposited on the original bird-beak tip using electron beam deposition (EBD), and sharpened by a plasma etching in an argon environment. The typical radius of the EBD tip was

approximately 2 nm after the sharpening. For the tapping-mode imaging, the cantilever was oscillated with an amplitude of about 1 nm for the free oscillation, and the amplitude was reduced to be ~ 90 % of the free oscillation amplitude for a feedback control. As a sample substrate, we used mica surface treated with (3-amino)propyltriethoxysilane (APTES). After cleavage of a mica sheet with 1.5 mm in a diameter, APTES (Shin-Etsu Chemical) with a concentration of 0.01% was deposited on the mica surface. After 3-min incubation, the mica surface was thoroughly washed with pure water. The BBP trimer with a concentration of 0.5 μM was deposited on the APTES-mica and incubated for 3 min. After the incubation, the residual molecules were thoroughly washed with an observation buffer (50 mM HEPES-NaOH, pH 7.0). After the washing, the tip was approached, and the HS-AFM imaging was performed under the buffer solution.

References

1. K. Oikawa, S. Nakamura, T. Sonoyama, A. Ohshima, Y. Kobayashi, S. J. Takayama, Y. Yamamoto, S. Uchiyama, J. Hasegawa, and Y. Sambongi, *J. Biol. Chem.*, 2005, **280**, 5527–5532.
2. E. Arslan, H. Schulz, R. Zufferey, P. Kunzler, and L. Thony-Meyer, *Biochem. Biophys. Res. Commun.*, 1998, **251**, 744-747.
3. E. A. Berry, and B. L. Trumpower, *Anal. Biochem.*, 1987, **161**, 1–15.
4. K. Yoshizawa, Y. Mishima, S. Y. Park, J. G. Heddle, J. R. H. Tame, K. Iwahori, M. Kobayashi, and I. Yamashita, *J. Biochem.*, 2007, **142**, 707–713.
5. R. Nagarajan, A. Archana, A. M. Thangakani, S. Jemimah, D. Velmurugan, and M. M. Gromiha, *Bioinform. Biol. Insights*, 2016, **10**, 73–80.
6. Z. Otwinowski and W. Minor, *Methods Enzymol.*, 1997, **276**, 307–326.
7. A. T. Brunger, P. D. Adams, G. M. Clore, W. L. DeLano, P. Gros, R. W. Grosse-Kunstleve, J. S. Jiang, J. Kuszewski, M. Nilges, N. S. Pannu, R. J. Read, L. M. Rice, T. Simonson, and G. L. Warren, *Acta Crystallogr. D Biol. Crystallogr.*, 1998, **54**, 905–21.
8. P. Emsley, and K. Cowtan, *Acta Crystallogr. D Biol. Crystallogr.*, 2004, **60**, 2126–2132.

Table S1. DNA and amino acid sequences of BBP.

DNA sequence
gaattcATGCGCAAAAGCCTGTTGGCGATTCTGGCAGTGAGCTCTCTTGTGTTTTCG AGTGCCAGTTTTGCCGTAGATCCGGCTAAAGAAGCGATCATGAAACCGCAATTG ACCATGCTCAAAGGCTTATCCGATGCCGAACTGAAGGCGTTAGCAGACTTCATTC TGCGCATTGCGAAACAGGCGCAGGAAAAACAGCAGCAGGATGTGGCGAAAGCG ATCTTTCAGCAGAAAGGCTGTGGTTCATGCCATCAGGCTAACGTCGATACGGTTG GTCCTAGCCTGGCGAAGATTGCACAAGCGTATGCCGGAAAAGAGGACCAGCTG ATCAAATTCCTGAAAGGCGAAGCTCCAGCGATTTAAgtcgac
Amino acid sequence
MRKSLLAILAVSSLVFSSASFAVDPAKEAIMKPQLTMLKGLSDAELKALADFILRIAK QAQEKQQQDVAKAIFQQKGCGSCHQANVDTVGPSLAKIAQAYAGKEDQLIKFLKG EAPAI

[a]Val1−Ala35 and Asp44−Ile96 regions of BBP are represented in green and magenta, respectively. The DNA and amino acids of the inserted 9 amino acid residues are represented in light blue. The digestion sites of *Eco*R I and *Sal* I restriction enzymes are depicted in small letters. The periplasmic targeting signal DNA and amino acid sequences are underlined.

Table S2. Statistics of data collection and structure refinement of the BBP trimer (PDB ID: 5Z25).

Data collection	
X-ray source	SPring-8 (BL38B1)
Wavelength (Å)	1.0000
Space group	*F*432
Unit cell parameters	
a, *b*, *c* (Å)	153.8, 153.8, 153.8
α, β, γ (º)	90.0, 90.0, 90.0
Resolution (Å)	50.0−1.70 (1.73−1.70)
Number of unique reflections	17053 (871)
R_{merge}[a]	0.099 (1.121)
Completeness (%)	96.0 (100.0)
$\langle I/\sigma(I)\rangle$	23.8 (2.7)
$CC_{1/2}$	(0.894)
Redundancy	18.6 (19.6)

Refinement	
Resolution (Å)	50.0−1.70 (1.74−1.70)
Number of reflections	15942 (1281)
R_{work}[b]	0.2269 (0.205)
R_{free}[b]	0.2683 (0.254)
Completeness (%)	94.8 (100.0)
Number of atoms in an asymmetric unit	
Protein	723
Water	85
Heme	43
Average *B* factors (Å^2)	
Protein	19.9
Water	27.7
Heme	12.2
Ramachandran plot (%)	
Favored	97.87
Allowed	1.06
Outlier	1.06

Statistics for the highest-resolution shell are given in parentheses.

[a] $R_{merge}=\Sigma_{hkl} | I - \langle I\rangle | (\Sigma_{hkl}| I |)^{-1}$.

[b] $R_{work}=\Sigma_{hkl} | | F_{obs} | - k| F_{calc} | | (\Sigma_{hkl} | F_{obs} |)^{-1}$, k: scaling factor. R_{free} was computed identically, except where all reflections belong to a test set of 5 % of randomly selected data.

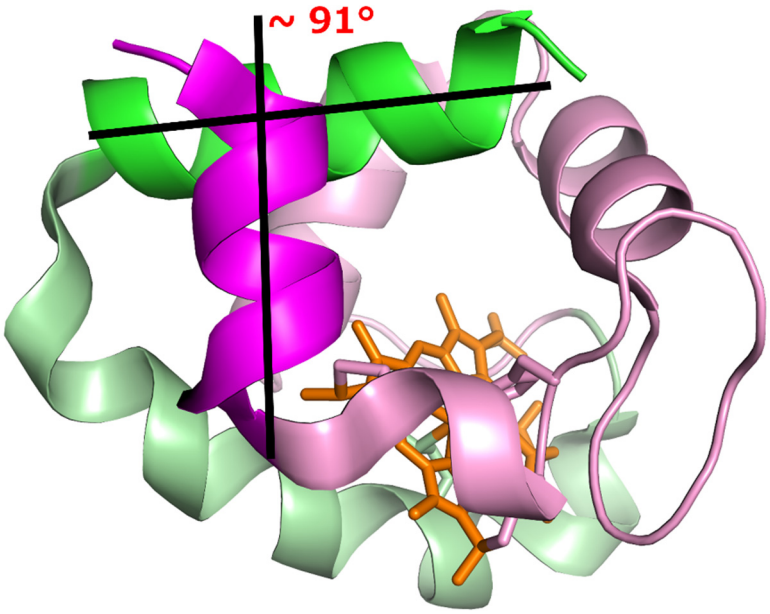

Figure S1. Interaction between the N- and C-terminal α-helices of AA cyt c_{555} with a defined angle (~ 91°). The N- and C-terminal regions are shown in magenta and green, respectively.

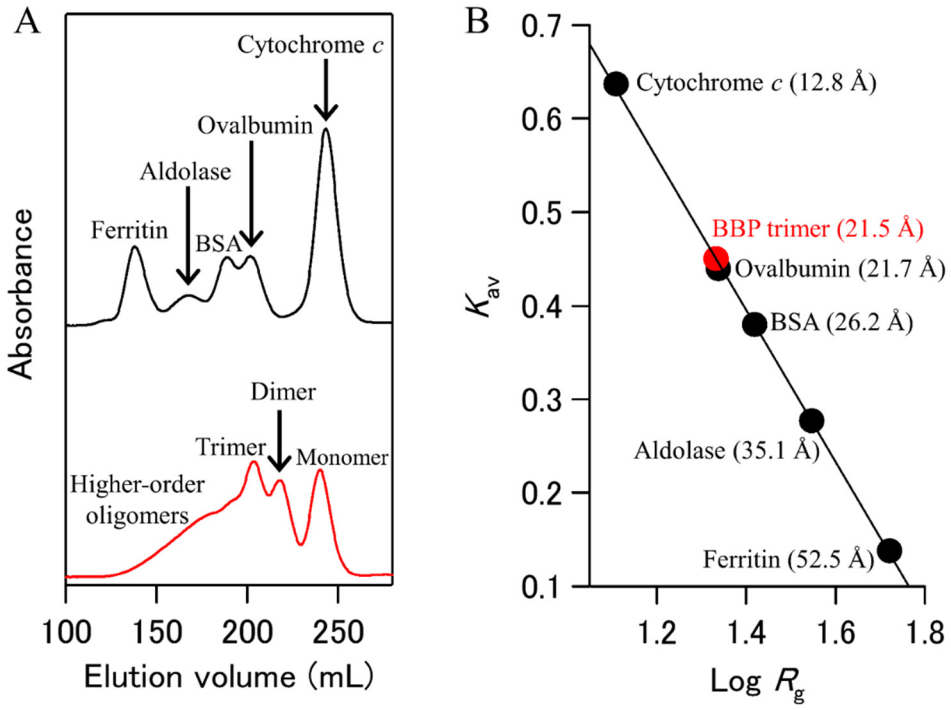

Figure S2. (A) Size exclusion chromatogram of BBP oligomers after drying the monomer solution at 80 ºC and re-dissolving the residual with pure water: BBP oligomers (red line); standard proteins (black line). The monomer and dimer of BBP may form by the inserted linker exhibiting a loop structure. (B) Calibration curve of the radius of gyration (R_g) for the column used. The calibration curve (black line) was obtained by least-square fitting the plots of logarithm of R_g against partition coefficient (K_{av}) for standard proteins (black circles); horse cytochrome *c* (12.8 Å), ovalbumin (21.7 Å), BSA (26.2 Å), aldolase (35.1 Å), and ferritin (52.5 Å). The BBP trimer plot (red circle) is depicted with its estimated R_g in parentheses. Experimental conditions: column, HiLoad 26/60 Superdex 200 pg; buffer, 50 mM potassium phosphate buffer, pH 7.0; monitoring wavelength, 280 nm.

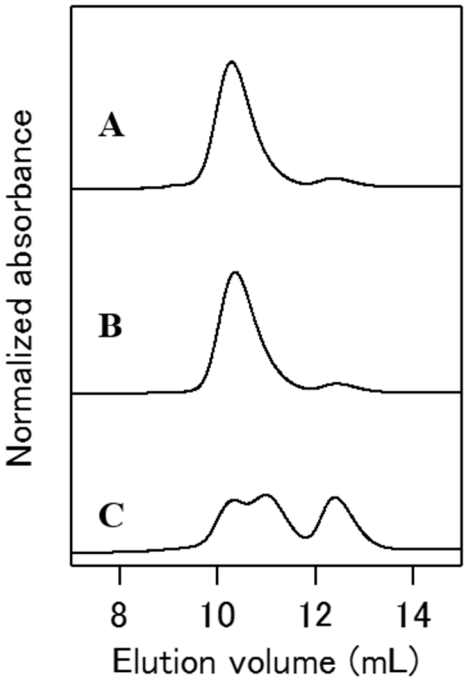

Figure S3. Size exclusion chromatograms of the BBP trimer (A) without incubation, or after incubation for 30 min at (B) 40 °C or (C) 50 °C. Measurement conditions: column, Superdex 75 10/300 GL; monitoring wavelength, 410 nm; buffer, 50 mM potassium phosphate buffer, pH 7.0; temperature, 4 °C. The intensities of the curves are normalized by the total area of the curve.

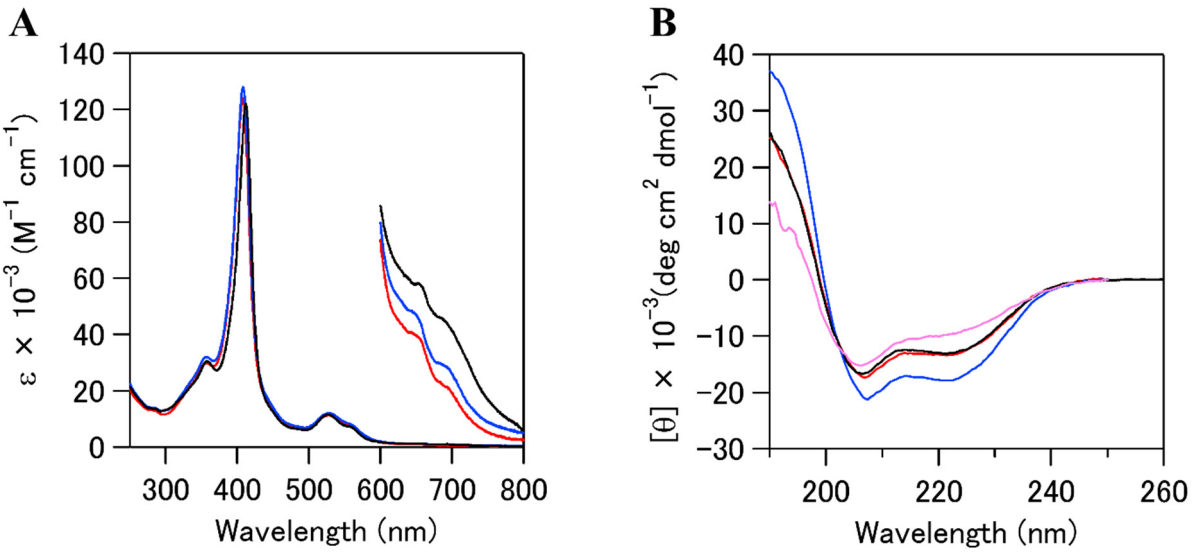

Figure S4. (A) Optical absorption and (B) CD spectra of AA cyt c_{555}, BBP monomer, and BBP trimer. The spectra of the BBP monomer at 25 and 100 °C are shown in red and pink, respectively. The spectra of AA cyt c_{555} and the BBP trimer are shown in black and blue, respectively. Measurement conditions: sample concentration, (A) 7 and 50 μM (7 μM, 250–800-nm region; 50 μM, 600–800-nm region) and (B) 18 μM; buffer, 50 mM potassium phosphate buffer; pH 7.0; temperature, AA cyt c_{555} and BBP trimer, 25 °C; BBP monomer, 25 and 100 °C.

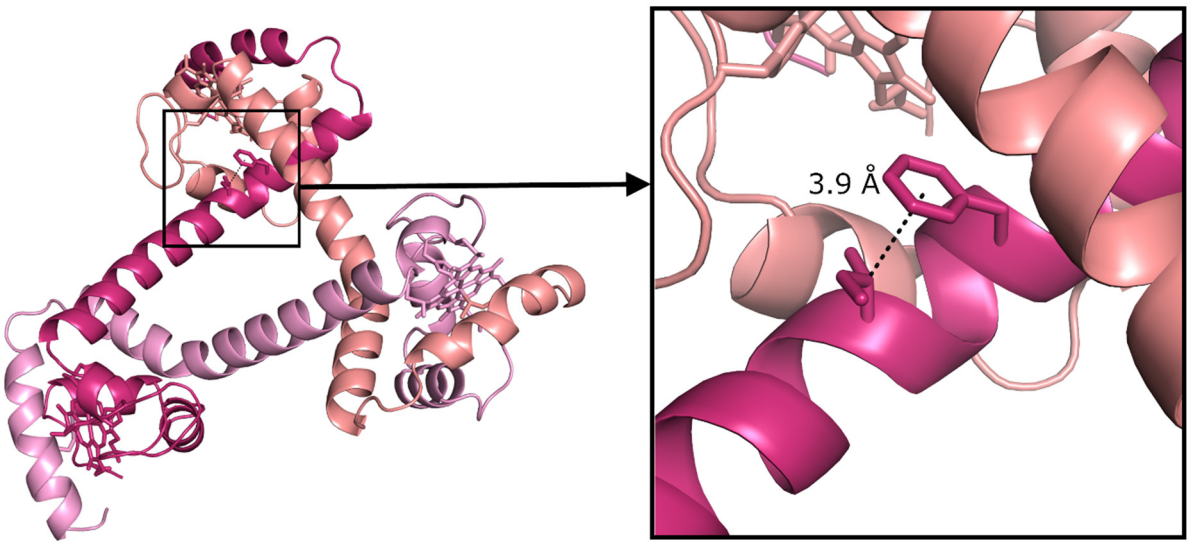

Figure S5. Bending region in the α-helix linker of the BBP trimer (PDB ID: 5Z25). Each protomer is shown in violet, red purple, and pink, respectively. The expanded figure of the CH−π interaction region in the BBP trimer is shown in the right. Phe30 and Ile34 exhibiting CH−π interaction are shown as stick models. The distance between the Cβ atom of Ile34 and the center of the aromatic ring of Phe30 is 3.9 Å.

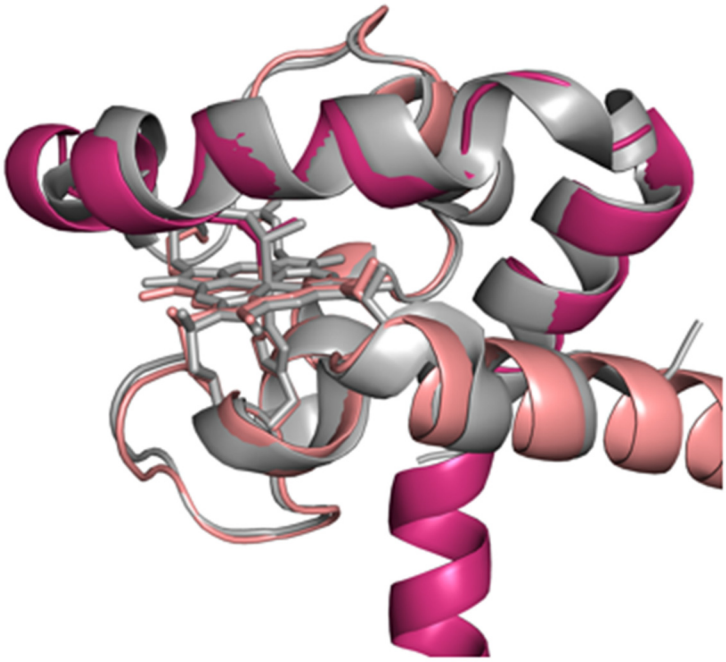

Figure S6. Overlapped view of the BBP trimer globular unit (PDB ID: 5Z25) and AA cyt c_{555} (PDB ID: 2ZXY) (gray). The two protomers of the BBP trimer are depicted in violet and pink, respectively. The hemes, Met and His coordinating to the hemes, and Cys covalently bound to the heme are shown as stick models.

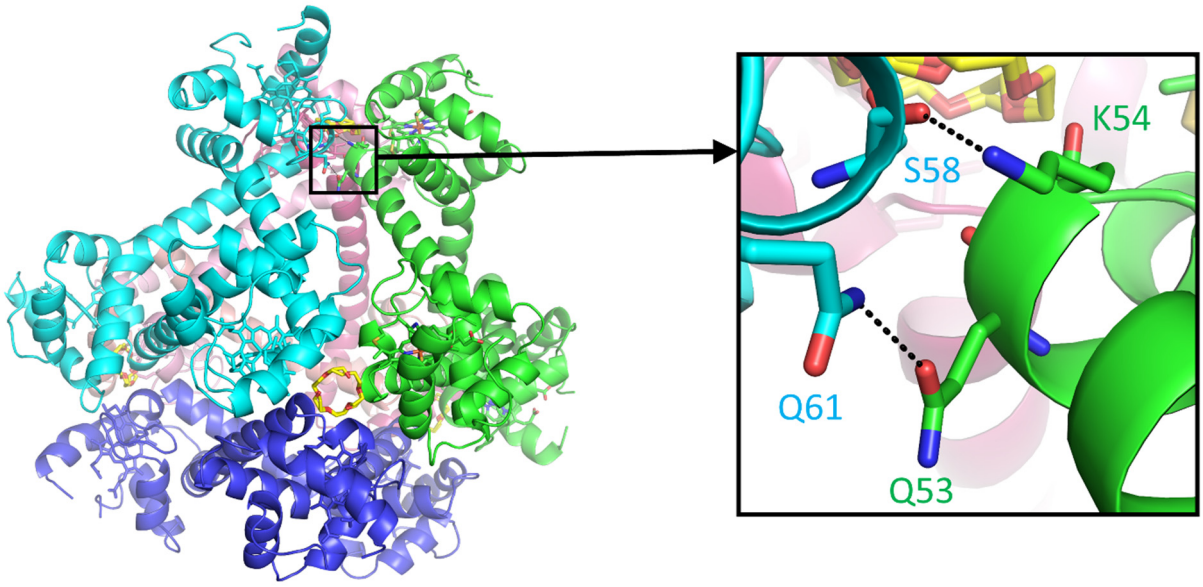

Figure S7. Hydrogen bonds between different BBP trimers of the tetrahedron (PDB ID: 5Z25). The expanded figure of the hydrogen bond region in the tetrahedron is shown in the right. The oxygen and nitrogen atoms are shown in red and blue, respectively. The distance between the Nζ atom of Lys54 (green) and the main chain O atom of Ser58 (cyan) is 3.0 Å, and that between the Oε1 atom of Gln53 (green) and the Nε2 atom of Gln61 (cyan) is 3.1 Å.

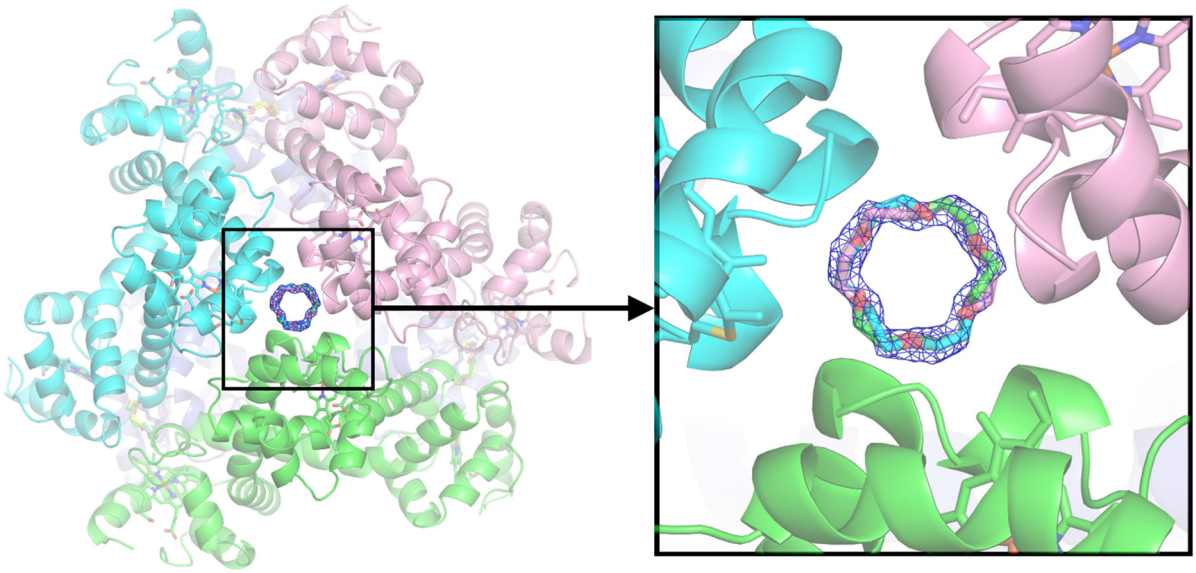

Figure S8. $F_o - F_c$ omit map of the PEG molecule ($C_8H_{18}O_5$) at the vertex of the tetrahedron constructed with four BBP trimers (PDB ID: 5Z25). The expanded figure of the PEG molecules in the tetrahedron is shown in the right. The omit map is shown as a blue mesh and contoured at 3.0 σ. The PEG molecule position was optimized with a 0.33 occupation for each trimer in the crystal structure. The PEG molecules are shown as green, cyan, and pink stick models.

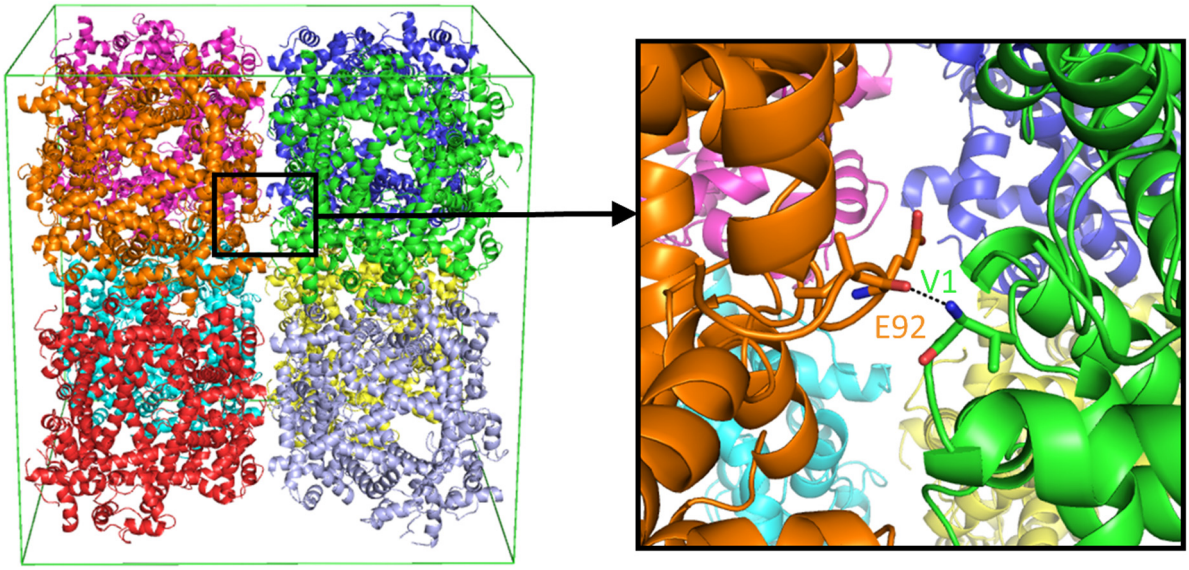

Figure S9. Packing of eight tetrahedrons in a unit cell (PDB ID: 5Z25). Each tetrahedron comprises four BBP trimers and is colored differently. The unit cell is shown in green lines. Forty-eight hydrogen bonds between Val1 of a trimer of a tetrahedron and Glu92 of a trimer of another tetrahedron are formed in the unit cell. An expanded figure of the hydrogen bond region is shown in the right. The nitrogen and oxygen atoms of a hydrogen bond are shown in blue and red, respectively. The distance between the main chain N atom of Val1 (green) and the main chain O atom of Glu92 (orange) is 2.7 Å.

Movie S1. HS-AFM movie of the BBP trimer on an APTES-treated mica substrate.